

A rapid monotonically convergent iteration algorithm for quantum optimal control over the expectation value of a positive definite operator

Cite as: J. Chem. Phys. **109**, 385 (1998); <https://doi.org/10.1063/1.476575>

Submitted: 03 October 1997 . Accepted: 31 March 1998 . Published Online: 29 June 1998

Wusheng Zhu, and Herschel Rabitz



View Online



Export Citation

ARTICLES YOU MAY BE INTERESTED IN

[Rapidly convergent iteration methods for quantum optimal control of population](#)

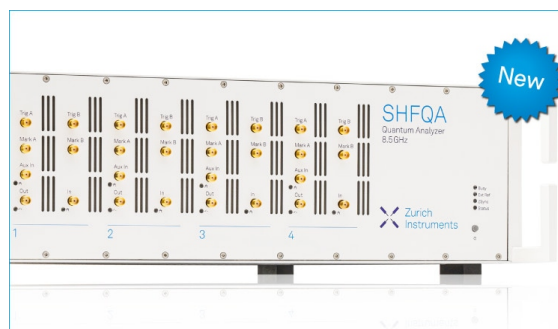
The Journal of Chemical Physics **108**, 1953 (1998); <https://doi.org/10.1063/1.475576>

[New formulations of monotonically convergent quantum control algorithms](#)

The Journal of Chemical Physics **118**, 8191 (2003); <https://doi.org/10.1063/1.1564043>

[Monotonically convergent algorithm for quantum optimal control with dissipation](#)

The Journal of Chemical Physics **110**, 9825 (1999); <https://doi.org/10.1063/1.478036>



Your Qubits. Measured.

Meet the next generation of quantum analyzers

- Readout for up to 64 qubits
- Operation at up to 8.5 GHz, mixer-calibration-free
- Signal optimization with minimal latency

Find out more



A rapid monotonically convergent iteration algorithm for quantum optimal control over the expectation value of a positive definite operator

Wusheng Zhu and Herschel Rabitz

Department of Chemistry, Princeton University, Princeton, New Jersey 08544-1009

(Received 3 October 1997; accepted 31 March 1998)

A new iteration method is presented for achieving quantum optimal control over the expectation value of a positive definite operator. Theoretical analysis shows that this new algorithm exhibits quadratic and monotonic convergence. Numerical calculations verify that for this new algorithm, within a few steps, the optimized objective functional comes close to its converged limit. © 1998 American Institute of Physics. [S0021-9606(98)01326-9]

I. INTRODUCTION

Optimal control theory provides a general framework for designing controls over molecular dynamics phenomena.¹⁻⁴ In its implementation, the variational procedure requires the solution of coupled nonlinear equations in which the optimal solution is embedded. Since different numerical methods can result in vastly different computational efforts to find the solutions, or even fail to converge, the determination of reliable and efficient numerical methods to solve the nonlinear equations is an important task. In recent years various numerical methods, including the conjugate gradient method^{2,3} and Krotov iteration method,⁴ were developed for solving the optimal control nonlinear equations. However, the reliability and/or the efficiency of these methods leave much to be desired. In this paper, we develop a special entangled feedback iteration method, which is superior to other methods in reliability and efficiency for solving the common optimal control problem of maximizing the expectation value of positive definite operators.

In a recent paper,⁵ we developed a new family of rapidly convergent algorithms to solve the problem of optimal control of population.⁶ As a further step, here we consider the more general problem of achieving quantum control over the expectation value of a positive definite operator by means of an external laser field while minimizing the laser energy. Consideration of a positive definite target operator should be adequate for many applications, although it is not fully general. The positive definite nature of the operator is necessary to obtain the property of monotonic convergence, as shown later. We construct the following objective functional, \mathbf{J}_{fi} , to be maximized and intend to develop a rapidly convergent method for its optimization:

$$\mathbf{J}_{fi} = \langle \psi_i(T) | O | \psi_i(T) \rangle - \alpha_0 \int_0^T [\epsilon(t)]^2 dt - 2 \operatorname{Re} \left[\int_0^T \langle \chi_f(t) | \frac{\partial}{\partial t} + i[H_0 + V - \mu \epsilon(t)] | \psi_i(t) \rangle dt \right], \quad (1)$$

where $\psi_i(t)$ is the wave function driven by the optimal laser field, $\epsilon(t)$. The initial wave function is $\psi_i(0) \equiv \varphi_i(0)$, and O is a positive definite operator at the final time T . α_0 is a

positive parameter chosen to weight the significance of the laser fluence. $\chi_f(t)$ can be regarded as a Lagrange multiplier introduced to assure satisfaction of the Schrödinger equation. In the Hamiltonian, H_0 is the kinetic operator, V is the potential energy, and μ is the transition dipole moment.

Requiring $\delta \mathbf{J}_{fi} = 0$ will give the equations satisfied by the wave function, Lagrange multiplier, and optimized laser field:⁶

$$i \frac{\partial}{\partial t} \psi_i(t) = [H_0 + V - \mu \epsilon(t)] \psi_i(t), \quad \psi_i(0) = \varphi_i(0), \quad (2)$$

$$i \frac{\partial}{\partial t} \chi_f(t) = [H_0 + V - \mu \epsilon(t)] \chi_f(t), \quad \chi_f(T) = O \psi_i(T), \quad (3)$$

$$\alpha_0 \epsilon(t) = -\operatorname{Im} \langle \chi_f(t) | \mu | \psi_i(t) \rangle. \quad (4)$$

Any $\epsilon(t)$ which satisfies the above three coupled equations [Eqs. (2)–(4)] would be a local optimal solution for the control problem. Substitution of Eq. (4) into Eqs. (2) and (3) gives the dynamical system to be solved:

$$i \frac{\partial}{\partial t} \psi_i(t) = (H_0 + V) \psi_i(t) + \frac{\mu}{\alpha_0} \psi_i(t) \operatorname{Im} \langle \chi_f(t) | \mu | \psi_i(t) \rangle, \quad (5)$$

$$\psi_i(0) = \varphi_i(0),$$

$$i \frac{\partial}{\partial t} \chi_f(t) = (H_0 + V) \chi_f(t) + \frac{\mu}{\alpha_0} \chi_f(t) \operatorname{Im} \langle \chi_f(t) | \mu | \psi_i(t) \rangle, \quad (6)$$

$$\chi_f(T) = O \psi_i(T).$$

In order to solve the above coupled nonlinear equations [Eqs. (5) and (6)], it is evident that iterative methods need to be employed. A simple iteration method based on solving the coupled Schrödinger equations by guessing an initial field to obtain $\psi_i(t)$ and then $\chi_f(t)$ and using them to calculate a new field for the next iteration, etc., usually does not converge, as verified in numerical calculations.

In Sec. II, we will develop a new iteration method which incorporates feedback from the control field in an entangled fashion other than the one-step-to-next-step feedback style of the Krotov method,⁷ and the one-cycle-to-next-cycle (one

cycle of iteration includes a number of steps) feedback style of gradient-type methods. In particular, the new method will be proved to have fast quadratic monotonic convergence behavior which contributes to its achieving quality results after only a few iterations.

II. ITERATION ALGORITHM

Now we consider a particular iteration algorithm for solving Eqs. (5) and (6). The iteration procedure is specified as follows.

Step 1:

$$i \frac{\partial}{\partial t} \psi_i^{(0)}(t) = (H_0 + V) \psi_i^{(0)}(t) - \mu \bar{\epsilon}(t) \psi_i^{(0)}(t), \quad (7)$$

$$i \frac{\partial}{\partial t} \chi_f^{(1)}(t) = (H_0 + V) \chi_f^{(1)}(t) + \frac{\mu}{\alpha_0} \chi_f^{(1)}(t) \times \text{Im} \langle \chi_f^{(1)}(t) | \mu | \psi_i^{(0)}(t) \rangle, \quad (8)$$

$$i \frac{\partial}{\partial t} \psi_i^{(1)}(t) = (H_0 + V) \psi_i^{(1)}(t) + \frac{\mu}{\alpha_0} \psi_i^{(1)}(t) \times \text{Im} \langle \chi_f^{(1)}(t) | \mu | \psi_i^{(1)}(t) \rangle. \quad (9)$$

Step 2:

$$i \frac{\partial}{\partial t} \chi_f^{(2)}(t) = (H_0 + V) \chi_f^{(2)}(t) + \frac{\mu}{\alpha_0} \chi_f^{(2)}(t) \times \text{Im} \langle \chi_f^{(2)}(t) | \mu | \psi_i^{(1)}(t) \rangle, \quad (10)$$

$$i \frac{\partial}{\partial t} \psi_i^{(2)}(t) = (H_0 + V) \psi_i^{(2)}(t) + \frac{\mu}{\alpha_0} \psi_i^{(2)}(t) \times \text{Im} \langle \chi_f^{(2)}(t) | \mu | \psi_i^{(2)}(t) \rangle. \quad (11)$$

Step 3:

$$i \frac{\partial}{\partial t} \chi_f^{(3)}(t) = (H_0 + V) \chi_f^{(3)}(t) + \frac{\mu}{\alpha_0} \chi_f^{(3)}(t) \times \text{Im} \langle \chi_f^{(3)}(t) | \mu | \psi_i^{(2)}(t) \rangle, \quad (12)$$

$$i \frac{\partial}{\partial t} \psi_i^{(3)}(t) = (H_0 + V) \psi_i^{(3)}(t) + \frac{\mu}{\alpha_0} \psi_i^{(3)}(t) \times \text{Im} \langle \chi_f^{(3)}(t) | \mu | \psi_i^{(3)}(t) \rangle, \quad (13)$$

where the boundary conditions for $\chi_f(t)$ in each step are

$$\chi_f^{(1)}(T) = O \psi_i^{(0)}(T), \quad (14)$$

$$\chi_f^{(2)}(T) = O \psi_i^{(1)}(T), \quad (15)$$

$$\chi_f^{(3)}(T) = O \psi_i^{(2)}(T). \quad (16)$$

\vdots

The corresponding control field at each iteration step can be written as

$$\bar{\epsilon}(t) = 0 \quad (\text{or another chosen function}),$$

$$\alpha_0 \epsilon^{(0)}(t) = -\text{Im} \langle \chi_f^{(1)}(t) | \mu | \psi_i^{(0)}(t) \rangle, \quad (17)$$

$$\alpha_0 \epsilon^{(1)}(t) = -\text{Im} \langle \chi_f^{(1)}(t) | \mu | \psi_i^{(1)}(t) \rangle, \quad (18)$$

$$\alpha_0 \epsilon^{(2)}(t) = -\text{Im} \langle \chi_f^{(2)}(t) | \mu | \psi_i^{(1)}(t) \rangle, \quad (19)$$

$$\alpha_0 \epsilon^{(3)}(t) = -\text{Im} \langle \chi_f^{(2)}(t) | \mu | \psi_i^{(2)}(t) \rangle, \quad (20)$$

$$\alpha_0 \epsilon^{(4)}(t) = -\text{Im} \langle \chi_f^{(3)}(t) | \mu | \psi_i^{(2)}(t) \rangle, \quad (21)$$

$$\alpha_0 \epsilon^{(5)}(t) = -\text{Im} \langle \chi_f^{(3)}(t) | \mu | \psi_i^{(3)}(t) \rangle \quad (22)$$

\vdots

III. CONVERGENCE BEHAVIOR OF THE ITERATION ALGORITHM

After the first iteration step, the objective functional can be calculated by

$$\mathbf{J}_{fi}^{(0)} = \langle \psi_i^{(1)}(T) | O | \psi_i^{(1)}(T) \rangle - \alpha_0 \int_0^T [\epsilon^{(1)}(t)]^2 dt. \quad (23)$$

Similarly, after the second iteration step, the objective functional is

$$\mathbf{J}_{fi}^{(1)} = \langle \psi_i^{(2)}(T) | O | \psi_i^{(2)}(T) \rangle - \alpha_0 \int_0^T [\epsilon^{(3)}(t)]^2 dt. \quad (24)$$

Therefore, we can evaluate the deviation of the objective functional between the two iteration steps:

$$\begin{aligned} \delta \mathbf{J}_{10} &\equiv \mathbf{J}_{fi}^{(1)} - \mathbf{J}_{fi}^{(0)} \\ &= \langle \psi_i^{(1)}(T) + \delta \psi_{21}(T) | O | \psi_i^{(1)}(T) + \delta \psi_{21}(T) \rangle \\ &\quad - \langle \psi_i^{(1)}(T) | O | \psi_i^{(1)}(T) \rangle \\ &\quad - \alpha_0 \int_0^T ([\epsilon^{(3)}(t)]^2 - [\epsilon^{(1)}(t)]^2) dt, \end{aligned} \quad (25)$$

where $\delta \psi_{21}(T)$ is defined as $\delta \psi_{21}(T) \equiv \psi_i^{(2)}(T) - \psi_i^{(1)}(T)$. It can be further simplified to be

$$\begin{aligned} \delta \mathbf{J}_{10} &= 2 \text{Re} \langle \psi_i^{(1)}(T) | O | \delta \psi_{21}(T) \rangle + \langle \delta \psi_{21}(T) | O | \delta \psi_{21}(T) \rangle \\ &\quad - \alpha_0 \int_0^T ([\epsilon^{(3)}(t)]^2 - [\epsilon^{(1)}(t)]^2) dt \\ &= 2 \text{Re} \langle \chi_f^{(2)}(T) | \delta \psi_{21}(T) \rangle + \langle \delta \psi_{21}(T) | O | \delta \psi_{21}(T) \rangle \\ &\quad - \alpha_0 \int_0^T ([\epsilon^{(3)}(t)]^2 - [\epsilon^{(1)}(t)]^2) dt. \end{aligned} \quad (26)$$

During the iteration, we have

$$i \frac{\partial}{\partial t} \psi_i^{(1)}(t) = [H_0 + V - \mu \epsilon^{(1)}(t)] \psi_i^{(1)}(t), \quad (27)$$

$$i \frac{\partial}{\partial t} \psi_i^{(2)}(t) = [H_0 + V - \mu \epsilon^{(3)}(t)] \psi_i^{(2)}(t). \quad (28)$$

Subtracting Eq. (28) from Eq. (27), we obtain the equation for $\delta \psi_{21}(t) \equiv \psi_i^{(2)}(t) - \psi_i^{(1)}(t)$:

$$\begin{aligned}
i \frac{\partial}{\partial t} \delta\psi_{21}(t) &= [H_0 + V] \delta\psi_{21}(t) - \mu \epsilon^{(3)}(t) \psi_i^{(2)}(t) \\
&\quad + \mu \epsilon^{(1)}(t) \psi_i^{(1)}(t) \\
&= [H_0 + V - \mu \epsilon^{(2)}(t)] \delta\psi_{21}(t) \\
&\quad - \mu [\epsilon^{(3)}(t) - \epsilon^{(2)}(t)] \psi_i^{(2)}(t) \\
&\quad - \mu [\epsilon^{(2)}(t) - \epsilon^{(1)}(t)] \psi_i^{(1)}(t). \quad (29)
\end{aligned}$$

The formal solution of Eq. (29) is

$$\begin{aligned}
\delta\psi_{21}(t) &= \mathbf{T} \exp\left(-i \int_0^t [H_0 + V - \mu \epsilon^{(2)}(\tau)] d\tau\right) \\
&\quad \times \int_0^t \mathbf{T} \exp\left(i \int_0^{\tau'} [H_0 + V - \mu \epsilon^{(2)}(\tau)] d\tau\right) \\
&\quad \times i \mu [\epsilon^{(3)}(\tau') - \epsilon^{(2)}(\tau')] \psi_i^{(2)}(\tau') \\
&\quad + [\epsilon^{(2)}(\tau') - \epsilon^{(1)}(\tau')] \psi_i^{(1)}(\tau') d\tau', \quad (30)
\end{aligned}$$

where \mathbf{T} is the time ordering operator. Denoting

$$U(t, 0, \epsilon^{(2)}) \equiv \mathbf{T} \exp\left(-i \int_0^t [H_0 + V - \mu \epsilon^{(2)}(\tau)] d\tau\right) \quad (31)$$

we rewrite Eq. (30) as

$$\begin{aligned}
\delta\psi_{21}(t) &= i U(t, 0, \epsilon^{(2)}) \int_0^t U^\dagger(t', 0, \epsilon^{(2)}) \\
&\quad \times \mu [\epsilon^{(3)}(t') - \epsilon^{(2)}(t')] \psi_i^{(2)}(t') \\
&\quad + [\epsilon^{(2)}(t') - \epsilon^{(1)}(t')] \psi_i^{(1)}(t') dt'. \quad (32)
\end{aligned}$$

Setting $t = T$ in Eq. (32) and inserting it into Eq. (26), we will obtain

$$\begin{aligned}
\delta\mathbf{J}_{10} &= 2 \operatorname{Re} i \left\langle \chi_f^{(2)}(T) \middle| U(T, 0, \epsilon^{(2)}) \int_0^T U^\dagger(t, 0, \epsilon^{(2)}) \right. \\
&\quad \times \mu [\epsilon^{(3)}(t) - \epsilon^{(2)}(t)] \psi_i^{(2)}(t) \\
&\quad \left. + [\epsilon^{(2)}(t) - \epsilon^{(1)}(t)] \psi_i^{(1)}(t) dt \right\rangle \\
&\quad + \langle \delta\psi_{21}(T) | O | \delta\psi_{21}(T) \rangle \\
&\quad - \alpha_0 \int_0^T ([\epsilon^{(3)}(t)]^2 - [\epsilon^{(1)}(t)]^2) dt. \quad (33)
\end{aligned}$$

According to Eqs. (10) and (19), it follows that

$$\chi_f^{(2)}(t) = U(t, 0, \epsilon^{(2)}) U^\dagger(T, 0, \epsilon^{(2)}) \chi_f^{(2)}(T), \quad (34)$$

thereby simplifying Eq. (33) into

$$\begin{aligned}
\delta\mathbf{J}_{10} &= \int_0^T 2 \operatorname{Re} i \langle \chi_f^{(2)}(t) | \mu [\epsilon^{(3)}(t) - \epsilon^{(2)}(t)] \psi_i^{(2)}(t) \\
&\quad + [\epsilon^{(2)}(t) - \epsilon^{(1)}(t)] \psi_i^{(1)}(t) dt \rangle \\
&\quad + \langle \delta\psi_{21}(T) | O | \delta\psi_{21}(T) \rangle \\
&\quad - \alpha_0 \int_0^T ([\epsilon^{(3)}(t)]^2 - [\epsilon^{(1)}(t)]^2) dt. \quad (35)
\end{aligned}$$

Considering the expressions for control field in Eqs. (19) and (20), we finally have

$$\begin{aligned}
\delta\mathbf{J}_{10} &= 2 \alpha_0 \int_0^T (\epsilon^{(3)}(t) [\epsilon^{(3)}(t) - \epsilon^{(2)}(t)] \\
&\quad + \epsilon^{(2)}(t) [\epsilon^{(2)}(t) - \epsilon^{(1)}(t)]) dt \\
&\quad - \alpha_0 \int_0^T ([\epsilon^{(3)}(t)]^2 - [\epsilon^{(1)}(t)]^2) dt \\
&\quad + \langle \delta\psi_{21}(T) | O | \delta\psi_{21}(T) \rangle \\
&= \alpha_0 \int_0^T ([\epsilon^{(3)}(t) - \epsilon^{(2)}(t)]^2 + [\epsilon^{(2)}(t) - \epsilon^{(1)}(t)]^2) dt \\
&\quad + \langle \delta\psi_{21}(T) | O | \delta\psi_{21}(T) \rangle \\
&= \alpha_0 \int_0^T (|\delta\epsilon_{32}(t)|^2 + |\delta\epsilon_{21}(t)|^2) dt \\
&\quad + \langle \delta\psi_{21}(T) | O | \delta\psi_{21}(T) \rangle, \quad (36)
\end{aligned}$$

where $\delta\epsilon_{k+1,k}(t) \equiv \epsilon^{(k+1)}(t) - \epsilon^{(k)}(t)$. Since O is a positive definite operator, we have

$$\langle \delta\psi_{21}(T) | O | \delta\psi_{21}(T) \rangle \geq 0 \quad (37)$$

for all $\delta\psi_{21}(T) \neq 0$. Consequently, the deviation of the objective functional is proved to be non-negative:

$$\delta\mathbf{J}_{10} \geq 0, \quad (38)$$

where the equal sign occurs only if the initial guess happens to be the exact solution [i.e., $\delta\psi_{21}(t) = 0$]. Similarly, we can derive the deviation of the objective functional between two successive iteration steps:

$$\begin{aligned}
\delta\mathbf{J}_{N,N-1} &= \alpha_0 \int_0^T (|\delta\epsilon_{2N+1,2N}(t)|^2 + |\delta\epsilon_{2N,2N-1}(t)|^2) dt \\
&\quad + \langle \delta\psi_{N+1,N}(T) | O | \delta\psi_{N+1,N}(T) \rangle. \quad (39)
\end{aligned}$$

Then the total deviation of the objective functional is

$$\begin{aligned}
\delta\mathbf{J}_{N0} &= \alpha_0 \int_0^T \sum_{k=1}^{2N} |\delta\epsilon_{k+1,k}|^2 dt \\
&\quad + \sum_{k=1}^N \langle \delta\psi_{k+1,k}(T) | O | \delta\psi_{k+1,k}(T) \rangle. \quad (40)
\end{aligned}$$

Examination of Eq. (40) shows that the algorithm has bounded variational character with the following properties.

(i) The iteration sequence converges monotonically and quadratically in terms of the neighboring field deviations if O is a positive definite (or even only positive semidefinite) operator.

tor. (ii) Since the optimal control problem is designed for maximizing the objective functional, a larger deviation of the field between neighboring steps will lead to faster convergence of the objective functional. The initial trial field $\bar{\epsilon}(t)$ will typically be far from the exact solution, and thus we expect that the first few iteration steps will give the major contribution to the rapid convergence of the cost functional. However, the same logic suggests that the fractional rate of convergence will slow down after the initial high gain.

IV. DISCRETE IMPLEMENTATION OF THE ALGORITHM

In practice, we must choose an appropriate discrete propagation method to evaluate the algorithm. A simple approach would adopt the first-order split-operator method, which has some similar features to the Krotov method.⁷ But for higher efficiency, we employ a propagation method based on the second-order split-operator technique.

Step 1:

$$\begin{aligned}\psi_i^{(0)}(t_0 + \Delta t) &= e^{-iH_0\Delta t/2} e^{-i[V - \mu\bar{\epsilon}(t_0 + \Delta t/2)]\Delta t} \\ &\times e^{-iH_0\Delta t/2} \psi_i^{(0)}(t_0),\end{aligned}\quad (41)$$

$$\psi_i^{(0)}(0) = \varphi_i(0);$$

$$\begin{aligned}\chi_f^{(1)}(t_0 - \Delta t) &= e^{iH_0\Delta t/2} e^{i[V - \mu\epsilon^{(0)}(t_0 - \Delta t/2)]\Delta t} \\ &\times e^{iH_0\Delta t/2} \chi_f^{(1)}(t_0), \\ \epsilon^{(0)}(t_0 - \Delta t/2) &= -\frac{1}{\alpha_0} \text{Im}\langle \chi_f^{(1)}(t_0) | \mu \\ &+ \frac{i\Delta t}{2} [\mu, H_0] | \psi_i^{(0)}(t_0) \rangle,\end{aligned}\quad (42)$$

$$\chi_f^{(1)}(T) = O\psi_i^{(0)}(T);$$

$$\begin{aligned}\psi_i^{(1)}(t_0 + \Delta t) &= e^{-iH_0\Delta t/2} e^{-i[V - \mu\epsilon^{(1)}(t_0 + \Delta t/2)]\Delta t} \\ &\times e^{-iH_0\Delta t/2} \psi_i^{(1)}(t_0), \\ \epsilon^{(1)}(t_0 + \Delta t/2) &= -\frac{1}{\alpha_0} \text{Im}\langle \chi_f^{(1)}(t_0) | \mu \\ &- \frac{i\Delta t}{2} [\mu, H_0] | \psi_i^{(1)}(t_0) \rangle,\end{aligned}\quad (43)$$

$$\psi_i^{(1)}(0) = \varphi_i(0).$$

Step 2:

$$\begin{aligned}\chi_f^{(2)}(t_0 - \Delta t) &= e^{iH_0\Delta t/2} e^{i[V - \mu\epsilon^{(2)}(t_0 - \Delta t/2)]\Delta t} \\ &\times e^{iH_0\Delta t/2} \chi_f^{(2)}(t_0), \\ \epsilon^{(2)}(t_0 - \Delta t/2) &= -\frac{1}{\alpha_0} \text{Im}\langle \chi_f^{(2)}(t_0) | \mu \\ &+ \frac{i\Delta t}{2} [\mu, H_0] | \psi_i^{(1)}(t_0) \rangle,\end{aligned}\quad (44)$$

$$\chi_f^{(2)}(T) = O\psi_f^{(1)}(T);$$

$$\begin{aligned}\psi_i^{(2)}(t_0 + \Delta t) &= e^{-iH_0\Delta t/2} e^{-i[V - \mu\epsilon^{(3)}(t_0 + \Delta t/2)]\Delta t} \\ &\times e^{-iH_0\Delta t/2} \psi_i^{(2)}(t_0), \\ \epsilon^{(3)}(t_0 + \Delta t/2) &= -\frac{1}{\alpha_0} \text{Im}\langle \chi_f^{(2)}(t_0) | \mu \\ &- \frac{i\Delta t}{2} [\mu, H_0] | \psi_i^{(2)}(t_0) \rangle,\end{aligned}\quad (45)$$

$$\psi_i^{(3)}(0) = \varphi_i(0);$$

\vdots ,

where we have considered the Taylor expansion of the laser field up to first order:

$$\epsilon(t + \delta t) = \epsilon(t) + \frac{\partial \epsilon(t)}{\partial t} \delta t. \quad (46)$$

Roughly, in order to reach the same accuracy, a time step in the second-order scheme of Eqs. (41)–(45) can be ten times larger than that in the first-order scheme, while each iteration step in the second-order scheme will cost about twice as much as that in the first-order scheme. Thus, we anticipate that the efficiency of the second-order scheme will be about five times higher than that of the first-order scheme, which was verified in numerical tests.

V. NUMERICAL TESTS OF CONVERGENCE BEHAVIOR

In order to demonstrate the efficiency of the algorithm, we choose a typical one-dimensional test system consisting of the excitation from the ground state to a certain target in a Morse potential of the O–H bond. A positive definite operator O , denoted as $O(x)$ in the coordinate representation, is chosen to be

$$O(x) = \frac{\gamma_0}{\sqrt{\pi}} e^{-\gamma_0^2(x-x')^2}, \quad (47)$$

where γ_0 and x' are constants. Then the corresponding objective functional (also subject to the variational constraint term on the Schrödinger equation) to be maximized is

$$\begin{aligned}\mathbf{J}_{fi} &= \langle \psi_i(T) | O(x) | \psi_i(T) \rangle - \alpha_0 \int_0^T [\epsilon(t)]^2 dt \\ &= \int |\psi_i(x, T)|^2 \frac{\gamma_0}{\sqrt{\pi}} e^{-\gamma_0^2(x-x')^2} dx - \alpha_0 \int_0^T [\epsilon(t)]^2 dt.\end{aligned}\quad (48)$$

Since we have the asymptotic relation

$$\delta(x-x') = \lim_{\gamma \rightarrow \infty} \frac{\gamma}{\sqrt{\pi}} e^{-\gamma^2(x-x')^2}, \quad (49)$$

where δ is Dirac delta function, if γ_0 is chosen to be sufficiently large, the objective functional approaches

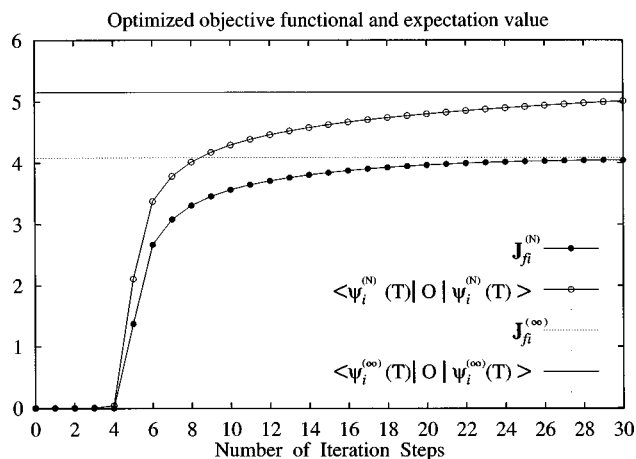


FIG. 1. Convergence of optimized objective functional $J_{fi}^{(N)}$ and expectation value $\langle \psi_i^{(N)}(T) | O | \psi_i^{(N)}(T) \rangle$ vs the number of iteration steps. The symbol ∞ denotes the observed final value after sufficient iteration steps. Rapid monotonic convergence is found.

$$J_{fi} \approx |\psi_i(x', T)|^2 - \alpha_0 \int_0^T [\epsilon(t)]^2 dt. \quad (50)$$

Therefore, the control problem is to maximize the probability distribution of the wave function at the position, $x=x'$, with the laser energy as the penalty. In the following calculations, all the parameters are expressed in atomic units (a.u.). The Morse potential⁸

$$V(x) = D_0 [e^{-\beta(x-x_0)} - 1]^2 - D_0 \quad (51)$$

has the parameters $D_0=0.1994$, $\beta=1.189$, $x_0=1.821$, and the dipole moment function is taken as⁹

$$\mu(x) = \mu_0 x e^{-x/x^*}, \quad (52)$$

where $\mu_0=3.088$, $x^*=0.6$. The initial wave function, $\phi_i(0)$, is chosen to be the Morse ground state.¹⁰ γ_0 and x' in the approximate Dirac delta function are chosen to be 25.0 and 2.5, respectively, and the final time is $T=131\,072$ a.u.

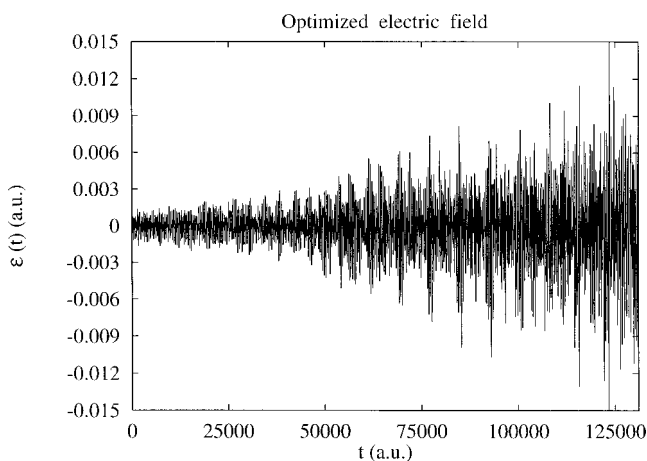


FIG. 2. Optimized electric field as a function of time. It is an interference pattern arising from many frequency components.

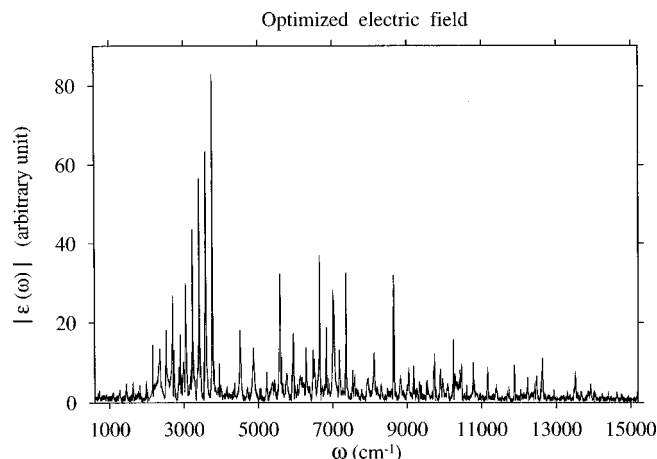


FIG. 3. Absolute value of the optimized electric field as a function of frequency. The major frequencies match bound state resonance conditions.

$T=131\,072$ a.u. (~ 3.167 ps). The trial input field is taken as $\bar{\epsilon}(t)=0$ and the penalty factor is $\alpha_0=1$.

Figure 1 shows the convergence behavior of the objective functional as well as the optimized expectation value versus the number of iteration steps. After seven iteration steps, the optimized objective functional is approximately 80% of its maximum value. Several more iteration steps are needed here compared to the previous case⁵ of population control to achieve a similar accuracy, because in the present case the initial and final states have essentially no overlap. Considering this fact, the convergence of the algorithm is still very fast. The numerical calculation verifies the prediction from Eq. (40) that each additional iteration step monotonically improve the previous iteration step by adding a positive term, and the first few steps give the major contribution corresponding to rapid convergence behavior. The convergence behavior of the expectation value is similar to that of the objective functional, although there is no rigorous basis for this behavior. The converged optimized electric field shown in Fig. 2 is an interference pattern arising from many frequency components. The corresponding frequency distribution in Fig. 3 displays many peaks located at the reso-

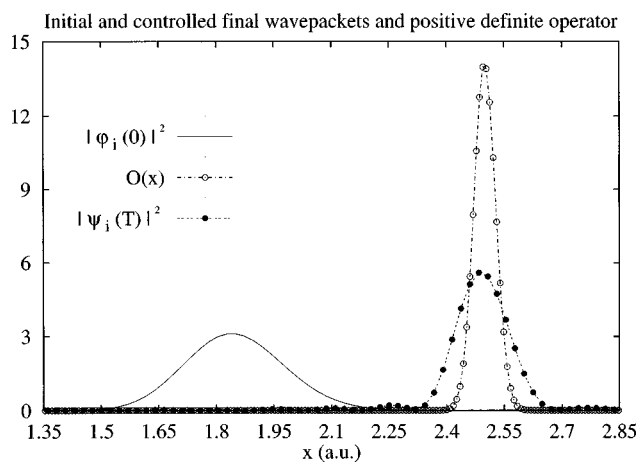


FIG. 4. Initial wave function $|\phi_i(0)|^2$, the positive definite operator $O(x)$, and the controlled wave function $|\psi_i(T)|^2$ at the final time.

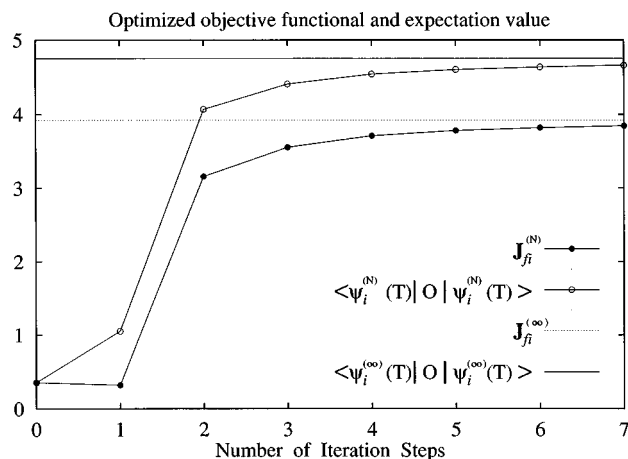


FIG. 5. Convergence of the optimized objective functional $J_{fi}^{(N)}$ and expectation value $\langle \psi_i^{(N)}(T) | O | \psi_i^{(N)}(T) \rangle$ vs the number of iteration steps. The symbol ∞ denotes the observed final value after sufficient iteration steps. Rapid monotonic convergence is found (where the values of the starting point at step "0" before iteration are just references and should be excluded in consideration of convergence behavior).

nant (including overtone excitation) frequencies of the Morse potential. This suggests that the control mechanism is to "synthesize" the final wave packet through many intermediate pathways. Many of the frequency components are small and likely could be eliminated if desired.

In Fig. 4 we display the square modulus of the initial wave function, the target function, and the controlled wave function at the final time. Good quality control is achieved (the goal is to make $|\psi_i(x, T)|^2$ peak around $x = x'$, not to make it appear like the target function). If the asymptotic potential energy $V(x \rightarrow \infty)$ is set to be zero, the energy of the initial eigenstate ($v = 0$) is -0.1904 a.u. taking into account the the zero point energy, $0.008\,994$ a.u., subtracted from the well depth, $D_0 = 0.1994$ a.u. For the optimized wave function which is not an eigenstate of the Morse potential, the average energy is $\langle \psi_i(T) | H | \psi_i(T) \rangle = -0.1141$ a.u. This energy is near that of the $v = 5$ eigenstate (-0.1126 a.u.).

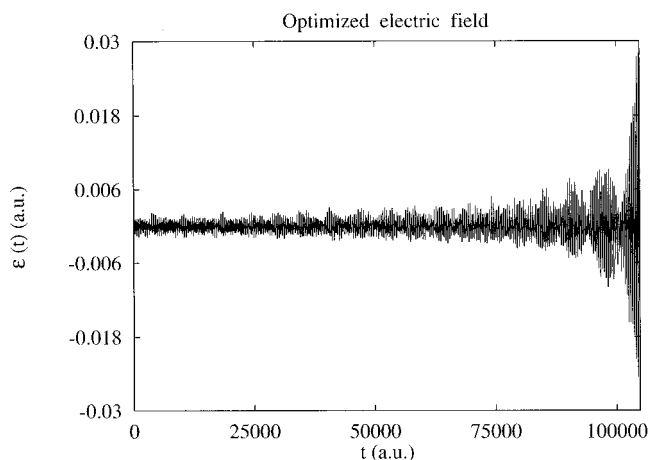


FIG. 6. Optimized electric field as a function of time. It is an interference pattern arising from many frequency components.

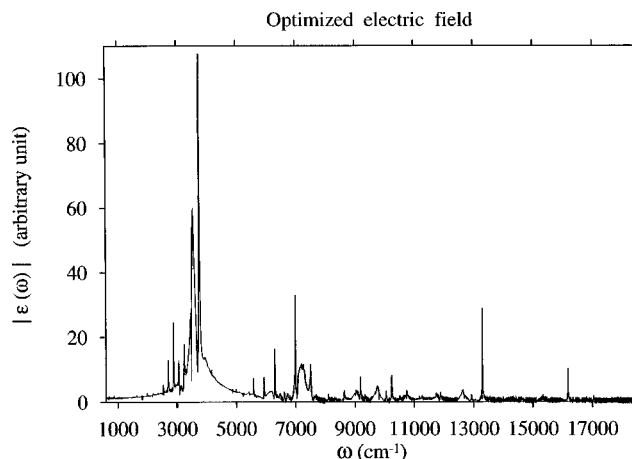


FIG. 7. Absolute value of the optimized electric field as a function of frequency. Most major frequencies match bound state resonance conditions.

In the second numerical example, we choose the initial wave function as the eigenstate of $v = 1$ in the aforementioned O–H oscillator. The positive definite operator is chosen to be a sharp Gaussian shape as described in Eq. (47) with a different location of the peak at $x' = x_0 = 1.821$ a.u. There are two major differences with the previous example. First, the target function overlaps with the initial function. Second, the initial function has two (multiple) peaks. The final time is set to $T = 104\,857.6$ a.u. (≈ 2.534 ps) and other parameters are set the same values as in the first example.

Figure 5 shows that only after two iteration steps, the optimized objective functional and expectation value are approximately 80% of their maximum values. Comparing with the convergence behavior in the previous example, we see that the convergence rate will be slower if the overlap between the initial and the target functions is weak. Figure 6 is the optimal electric field, which is an interference pattern arising from many frequency components. The power spectrum in Fig. 7 displays many peaks where the major components can be assigned to be resonant (including overtone excitation) frequencies of the Morse potential. The prominent frequency components are less than that in Fig. 3, which

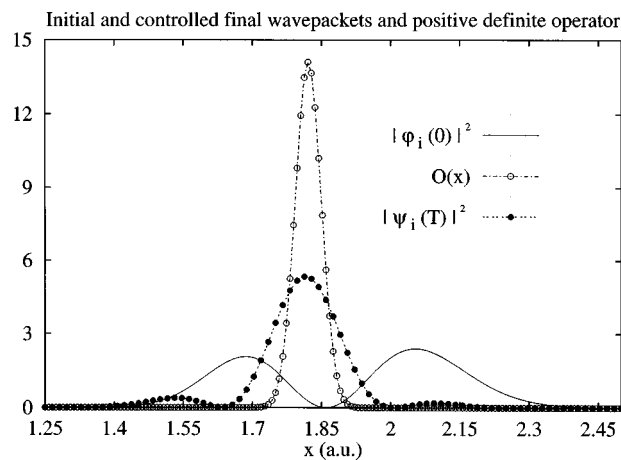


FIG. 8. Initial wave function $|\phi_i(0)|^2$, the positive definite operator $O(x)$, and the controlled wave function $|\psi_i(T)|^2$ at the final time.

is consistent with the control being relatively easier to achieve for the overlapping case. In Fig. 8 we display the square modulus of the initial function, the target positive definite operator, and the controlled wave function at the final time. The two original peaks are almost suppressed at the target time. The average energy of the controlled function, $\langle \psi_i(T) | H | \psi_i(T) \rangle = -0.1671$ a.u. lies between that of $v=1$ and $v=2$ eigenstates.

VI. SUMMARY

In this paper, we propose a new effective iteration method to solve quantum optimal control problems. The analysis shows that it is monotonically and quadratically convergent. In the first few iteration steps, the new method was found to converge to near 80% of its converged value.

ACKNOWLEDGMENTS

The authors acknowledge support from the National Science Foundation and the Army Research Office.

- ¹A. P. Pierce, M. A. Dahleh, and H. Rabitz, Phys. Rev. A **37**, 4950 (1988).
- ²S. Shi and H. Rabitz, Comput. Phys. Commun. **63**, 71 (1991).
- ³J. E. Combariza, B. Just, J. Manz, and G. K. Paramonov, J. Phys. Chem. **95**, 10351 (1991).
- ⁴J. Somloi, V. A. Kazakov, and D. J. Tannor, Chem. Phys. **172**, 85 (1993).
- ⁵W. Zhu, J. Botina, and H. Rabitz, J. Chem. Phys. **108**, 1953 (1998).
- ⁶S. Shi and H. Rabitz, J. Chem. Phys. **92**, 364 (1992).
- ⁷D. J. Tannor, V. A. Kazakov, and V. Orlov, in *Time-Dependent Quantum Molecular Dynamics*, edited by J. Broeckhove and L. Lathouwers (Plenum, New York, 1992).
- ⁸G. K. Paramonov, Chem. Phys. **177**, 169 (1993).
- ⁹R. T. Lawton and M. S. Child, Mol. Phys. **40**, 773 (1980).
- ¹⁰M. L. Sage, Chem. Phys. **35**, 375 (1978).